universe

IMPACT FACTOR 2.9

CITESCORE 3.6

Article

Role of Quark Matter and Color Superconductivity in the Structure and Tidal Deformability of Strange Dwarfs

Loïc Perot and Nicolas Chamel

Special Issue

Exotic Scenarios for Compact Astrophysical Objects

Edited by

Dr. Vlasios Petousis, Dr. Charalampos Moustakidis and Dr. Martin Veselsky

MDPI

https://doi.org/10.3390/universe9090382

universe

MDPI

Article

Role of Quark Matter and Color Superconductivity in the Structure and Tidal Deformability of Strange Dwarfs

Loïc Perot and Nicolas Chamel *

Institute of Astronomy and Astrophysics, CP-226, Université Libre de Bruxelles, 1050 Brussels, Belgium; loic.perot@ulb.be

* Correspondence: nicolas.chamel@ulb.be

Abstract: In 1995, Glendenning, Kettner and Weber postulated the existence of a new class of compact stars resembling white dwarfs but containing a small strange quark-matter core surrounded by hadronic layers attaining much higher densities than those found in white dwarfs. In our previous study, we have shown that it could be possible to unmask these so-called strange dwarfs through gravitational-wave observations with future space-based detectors such as the Laser Interferometer Space Antenna. We calculated more realistic equations of state for the hadronic envelope, but the quark core was treated using the simplest MIT bag model. In this paper, we investigate more closely the role of the possibly solid core in the structure and the tidal deformability of strange dwarfs in the full general relativistic framework by considering different models of strange quark matter in the crystalline color -superconducting phase. We find that the effect of the extreme rigidity of the elastic core on the tidal deformability is almost completely canceled by the surrounding hadronic layers. However, in all cases, the tidal deformability of strange dwarfs remains sufficiently lower than that of white dwarfs, to be potentially observable with gravitational waves despite the uncertainties in the strange quark-matter equation of state.

Keywords: quark matter; strange dwarf; white dwarf; color superconductivity; gravitational waves

Citation: Perot, L.; Chamel, N. Role of Quark Matter and Color Superconductivity in the Structure and Tidal Deformability of Strange Dwarfs. *Universe* **2023**, *9*, 382. https://doi.org/10.3390/universe9090382

Academic Editor: Banibrata Mukhopadhyay

Received: 14 July 2023
Revised: 11 August 2023
Accepted: 22 August 2023
Published: 25 August 2023

1. Introduction

As early as 1965, Ivanenko and Kurdgelaidze speculated that the core of neutron stars (NSs) is so dense that neutrons and protons could be crushed into free quarks. Soon afterwards, Itoh [1] calculated the structure of so-called strange stars (SSs) entirely made of strange quark matter, an admixture of up, down and strange quarks treated as degenerate Fermi gases. More realistic calculations were carried out by Brecher and Caporaso [2] using the MIT bag model, according to which quarks are confined inside a "bag" of the Quantum chromodynamics (QCD) vacuum [3]. In 1984, Witten [4] conjectured that strange quark matter could be produced $\sim 10^{-5}$ s after the Big Bang and could be the absolute ground state of matter (see also [5–7] for earlier studies about quark droplets). Alcock and collaborators pointed out that SSs could be surrounded by a very thin hadronic crust [8]. Later on, they proposed that white dwarfs (WDs) could also contain a quark core, leading to a new family of hybrid WDs [9]. Even more exotic objects, dubbed strange dwarfs (SDs), were postulated by Glendenning, Kettner and Weber [10,11] in 1995. The main particularity of these objects resembling WDs is that the hadronic region reaches higher densities than found in (hybrid) WDs. SDs are expected to be formed similarly to WDs, namely by the collapse of asymptotic giant branch stars, the only difference being that the progenitors had been accreting strange matter during their whole evolution [10]. The stability of SDs against radial perturbations was called into question by Alford and collaborators in 2017, casting doubt on the possible existence of these stars [12]. This issue has been further studied by other groups [13,14]: SDs have been shown to be stable if the conversions between quarks and hadrons are slower than the perturbations. We will assume that these conditions are fulfilled.

Although strange matter is not expected to have survived the extreme conditions prevailing in the primordial Universe [15], it could be also produced by the gravitational collapse of stellar cores during supernova explosions and be disseminated in the interstellar medium during the merger of NSs with another compact object [16]. Still, SSs and SDs have, up to now, remained elusive because of their close resemblance with NSs and WDs, respectively (potential candidates for SDs have been recently reported [17]). However, the situation may change in the coming years with the development of gravitational-wave (GW) astronomy. In particular, we have recently shown that it will be possible to identify SDs hidden in WD binaries through measurements of their tidal deformability with future space-based GW detectors, such as the Laser Interferometer Space Antenna (LISA) [18].

In [18], we have also developed a more realistic equation of state (EoS) for the description of the hadronic region of SDs, considering the compression of material made of the same light elements as found in WDs but undergoing electron captures and possibly pycnonuclear fusions. We have found that the internal constitution of SDs and their tidal deformability are markedly different from those obtained using the EoS of Baym, Pethick and Sutherland [19] adopted in most previous works and originally developed for the outer crust of NSs. For the quark core, we have used the simplest MIT bag model for massless and non interacting quarks [3]. The question therefore arises as to what extent our previous conclusions rely on the quark-matter properties. At asymptotically high densities, quark matter is predicted to be in a color-flavor-locked superconducting phase: up, down and strange quarks of all colors form zero-momentum spin singlet Cooper pairs based on the conventional Bardeen–Cooper–Schrieffer mechanism [20] (see, e.g., [21] for a review). At the comparatively much lower densities prevailing in the core of SDs, the actual phase of quark matter remains very uncertain. It has been proposed that the quark core is in a two-flavor color-superconducting phase [22], in which only the up and down quarks are paired. Alternatively, the core could be in a crystalline color-superconducting phase [23]. If so, the core would be extremely rigid: the shear modulus is predicted to be at least two or three orders of magnitude larger than that of the hadronic envelope [24].

As shown in [25,26], the high rigidity of the crystalline color-superconducting phase has a strong impact on the tidal deformability of bare SSs (inducing deviations up to 50%), but is partially canceled by the presence of a hadronic envelope. This screening effect increases with the relative thickness of the envelope in comparison with the core radius, but is reduced by the presence of a density discontinuity at the interface with the core. The results obtained in [25,26] for SSs cannot be directly translated to SDs because these two types of compact stars are very different. Not only do they differ in their size by 2–3 orders of magnitude ($\sim$10 km for SSs vs. $\sim$1000–10,000 km for SDs), but also in their internal constitution. Indeed, the envelope of SDs, which occupies most of the stellar interior, unlike SSs, is much less stratified than that of SSs and contains much lighter elements. Whether such screening effects are also present in SDs thus remains an open question.

In this work, we study more closely the role of quark matter and crystalline color superconductivity in the structure and tidal deformability of SDs. To this end, we solve Einstein's equations of general relativity perturbatively, including the elasticity of both the crust and the core considering different quark-matter EoSs together with realistic EoSs for the hadronic envelope presented in [18].

This paper is arranged as follow. The EoSs describing the interior of SDs are introduced in Section 2. After briefly reviewing the equations determining the global structure and tidal deformability of relativistic stars made of different layers in Section 3, numerical results are presented and analyzed in Section 4. Future prospects to potentially identify SDs with upcoming space-based GW detectors are discussed in our conclusions.

All values for the fundamental constants are taken from NIST CODATA 2018[1].

2. Equation of State of Strange Dwarfs

2.1. Hadronic Envelope

As discussed in [18], the hadronic region of an SD is expected to crystallize within a few billion years and to be stratified into different layers, each of which consists of a dense Coulomb plasma of atomic nuclei with charge number Z and mass number A embedded in a highly degenerate relativistic electron gas. Whereas the outermost envelope is presumably made of the same light element as in a WD, different elements are predicted to be present in the inner layers at pressures exceeding the limiting pressure P_β found in the core of the most massive WDs and marking the onset of electron captures by nuclei. At pressures $P > P_\beta$, nuclei might also undergo pycnonuclear fusion reactions. The highest possible pressure of the hadronic region is set by the neutron-drip pressure $P_{\rm drip}$, above which nuclei can emit free neutrons, which sink in the core and dissolve into quarks [8].

To a very good approximation, electrons can be treated as an ideal relativistic Fermi gas. We take into account corrections due to electrostatic interactions, electron exchange and electron charge polarization effects following [27]. The energy density $\mathcal{E}$ and the pressure P are then given by ($\hbar$ is the Planck–Dirac constant, α is the fine structure constant and c is the speed of light)

$$\begin{aligned}\mathcal{E} =& n_e \frac{M(A,Z)c^2}{Z} + \frac{m_e c^2}{8\pi^2 \lambda_e^3}\left[x_r(1+2x_r^2)\sqrt{1+x_r^2} - \ln\left(x_r + \sqrt{1+x_r^2}\right)\right]\left(1+\frac{\alpha}{2\pi}\right) \\ &+ C_M \left(\frac{4\pi}{3}\right)^{1/3} \alpha\hbar c n_e^{4/3} Z_{\rm eff}^{2/3} - n_e m_e c^2 \,, \end{aligned} \tag{1}$$

$$\begin{aligned}P =& \frac{m_e c^2}{8\pi^2 \lambda_e^3}\left[x_r\left(\frac{2}{3}x_r^2 - 1\right)\sqrt{1+x_r^2} + \ln\left(x_r + \sqrt{1+x_r^2}\right)\right]\left(1+\frac{\alpha}{2\pi}\right) \\ &+ \frac{C_M}{3}\left(\frac{4\pi}{3}\right)^{1/3} \alpha\hbar c n_e^{4/3} Z_{\rm eff}^{2/3} \,, \end{aligned} \tag{2}$$

where n_e is the electron number density, the ion mass $M(A,Z)$ (including the rest mass m_e of Z electrons) is obtained after subtracting out the electron-binding energy from the tabulated experimental *atomic* mass using Equation (A4) of [28], $x_r = \lambda_e k_e$ is a dimensionless relativity parameter, $\lambda_e = \hbar/(m_e c)$ is the electron Compton wavelength, $k_e = (3\pi^2 n_e)^{1/3}$ is the electron Fermi wave number, C_M is the Madelung constant characterizing the spatial arrangement of ions and the effective proton charge is given by

$$Z_{\rm eff} \equiv Z\left[1 + \alpha \frac{12^{4/3}}{35\pi^{1/3}}(1 - 1.1866\, Z^{-0.267} + 0.27\, Z^{-1}) Z^{2/3}\right]^{3/2} . \tag{3}$$

For nuclei crystallized into a body-centered cubic lattice, the Madelung constant is given by $C_M = -0.895929255682$ [29]. Treating the crust as a polycrystal at the scales of interest here, the effective shear modulus is given by [30]

$$\tilde{\mu} = \left(\frac{4\pi}{3}\right)^{1/3} \alpha\hbar c \left(0.119457234091 - 9.4 \times 10^{-4} Z^{2/3}\right) Z^{2/3} n_e^{4/3} \,. \tag{4}$$

Depending on the stellar evolution, the hadronic envelope of an SD exhibits different compositions and the pressure $P_{\rm cc}$ delimiting the crust–core interface varies between P_β and $P_{\rm drip}$. The properties of this envelope and its role in the structure and in the tidal deformability of SDs was extensively studied in [18]. Since the present work is aimed at understanding the influence of the quark core, we will focus on oxygen SDs, whose hadronic envelope consists of an outermost layer made of ^{16}O surrounding a thin layer of ^{16}C (see Table II in [18] for details). For comparison, we will consider WDs entirely made of ^{16}O and described by the same EoS.

2.2. Strange Matter Core

The core of SDs is described using a phenomenological model of strange quark matter for which the pressure P is related to the energy density $\mathcal{E}$ through the following EoS [31,32]:

$$P = \frac{1}{3}[\mathcal{E} - 4\mathcal{B}_{\rm eff}(\mathcal{E})]\,, \tag{5}$$

where we have introduced the effective bag function

$$\mathcal{B}_{\rm eff}(\mathcal{E}) = \mathcal{B} + \frac{3a_2}{8\pi^2(\hbar c)^3}\mu_q^2\,. \tag{6}$$

The first term in Equation (6) arises from the MIT bag model [3] for massless and non-interacting quarks, with $\mathcal{B}$ the bag constant representing the excess energy density of the QCD vacuum (this is the EoS we adopted in our previous study [18]). The second term is a correction arising from the strange quark mass m_s, color superconductivity and QCD interactions. The coefficient a_2 effectively accounts for the strange quark mass and color superconductivity. The square of the averaged quark chemical potential μ_q is given by

$$\mu_q^2 = \frac{1}{6a_4}\left(a_2 + \sqrt{a_2^2 + 16\pi^2 a_4(\hbar c)^3(\mathcal{E} - \mathcal{B})}\right), \tag{7}$$

where a_4 originates from the correction of the Fermi momentum due to the QCD coupling. To assess the impact of the uncertainties in the quark-matter EoS, we have considered two sets of parameters representing the two extreme situations presented in [33]: SD1 with $\mathcal{B} = 58$ MeV fm^{-3}, $a_2 = 0$, $a_4 = 0.7$, and SD2 with $\mathcal{B} = 96$ MeV fm^{-3}, $a_2 = (200\,\text{MeV})^2$, and $a_4 = 0.7$. We have also considered linear fits of different models discussed in [34]:

$$P = c_s^2\,(\rho - \rho_s)\,, \tag{8}$$

where c_s represents the speed of sound, $\rho = \mathcal{E}/c^2$ the mass-energy density and ρ_s the excess mass-energy density of the QCD vacuum. Different parametrizations are listed in Table 1: SQM1 and SQM2 were calculated using the MIT bag model with massive strange quarks and QCD interactions for different sets of parameters [35] ($m_s = 200$ MeV/c^2, $\mathcal{B} = 56$ MeV fm^{-3} and QCD coupling constant $\alpha_s = 0.2$ for SQM1; $m_s = 100$ MeV/c^2, $\mathcal{B} = 40$ MeV fm^{-3} and $\alpha_s = 0.6$ for SQM2), whereas SS1 and SS2 were obtained within a vector-interaction model [36]. Note that for the simplest MIT bag model considered in our previous study, $(c_s/c)^2 = 1/3$ and $\rho_s = 4\mathcal{B}/c^2$.

Table 1. Parameters of Equation (8) for different models of quark matter [34].

Model	$(c_s/c)^2$	ρ_s [10^{14} g cm^{-3}]
SQM1	0.301	4.50
SQM2	0.324	3.06
SS1	0.463	11.54
SS2	0.455	13.32

The shear modulus of the core assumed to be in a crystalline color-superconducting phase is given by [24]

$$\tilde{\mu} = 2.47\ \text{MeV fm}^{-3}\left(\frac{\Delta}{10\ \text{MeV}}\right)^2\left(\frac{\mu_q}{400\ \text{MeV}}\right)^2. \tag{9}$$

The pairing gap of the crystalline color-superconducting phase is expected to lie in the range Δ = 5–25 MeV [24]. The core turns out to be much more rigid than the crust: the ratio $\tilde{\mu}/P$ is of the order $\sim$10, whereas it is of order $\sim 10^{-2}$ at the bottom of the hadronic region.

3. Structure and Tidal Deformability

The background structure of a spherically symmetric star in general relativity is described by the Tolman-Oppenheimer-Volkoff (TOV) equations relating the gravitational mass $m(r)$, the pressure $P(r)$ and the energy density $\mathcal{E}(r)$ as a function of the radial coordinate r. Solving these equations together with an EoS of the form $P = P(\mathcal{E})$ from the center of the star to the surface (at which point the pressure vanishes) provides the radius R and the total gravitational mass $M = m(R)$ of the star.

If an SD is in a close orbit with a compact companion, it gets tidally deformed by the mutual gravitational interactions. Assuming internal motions are much faster than orbital motions (adiabatic approximation), the static external quadrupolar tidal field $\mathcal{E}_{ij}$ induces a nonzero quadrupolar mass moment $\mathcal{Q}_{ij}$ in the SD, which is given to linear order by [37]

$$\mathcal{Q}_{ij} = \frac{2}{3G} k_2 R^5 \mathcal{E}_{ij} \,, \tag{10}$$

where G is the universal gravitational constant and the second gravitoelectric Love number k_2 is a dimensionless parameter characterizing the tidal response of the star. The tidal effects are described by the perturbed Einstein field equations:

$$\delta G^{\nu}_{\mu} = \frac{8\pi G}{c^4} (\delta T^{\nu}_{\mu} + \delta \Pi^{\nu}_{\mu}) \,, \tag{11}$$

where we have taken into account the elasticity of crystallized matter by adding the variations $\delta\Pi^{\nu}_{\mu}$ of the elastic shear tensor to the perfect-fluid contribution δT^{ν}_{μ}. Specifying the Eulerian static metric perturbation in the Regge–Wheeler gauge and the static Lagrangian displacement vector, one can compute and simplify Equation (11) to obtain a system of six ordinary first-order differential equations to be solved numerically inside the star together with the TOV equations. The full set of equations is given in [38]. Initial conditions at the star center are given by the Taylor expansions of the different functions, and appropriate boundary conditions are imposed at the crust–core interface and at transitions between adjacent hadronic layers marked by density and shear modulus discontinuities (see [38] for details). Finally, matching the results at the stellar surface with the exterior solution of the perturbed equations (in the vacuum) determines the tidal Love number k_2. Note that elasticity has no effect on the stellar radius or on the mass, since it comes into play at the perturbed level only.

4. Numerical Results

In this section, we present results obtained by numerically solving the equations for the structure and the tidal deformability of a compact star in full general relativity introduced in Section 3, taking into account the elasticity of the different regions and using the EoSs described in Section 2.

4.1. Numerical Scheme

Since we assumed that the entire SD was solid, we integrated the elastic system of differential equations for the tidal perturbations from a small value of the radial coordinate (to avoid singularities at the stellar center) up to the crust–core interface. We used the Taylor expansions of the different functions as initial conditions, and we generated three linearly-independent solutions, as detailed in [38]. In this situation, and contrary to the SD models with a fluid core presented in [18], it was convenient to perform the integration in the hadronic envelope inward. Indeed, the superposition of the different solutions at the stellar surface proved to be numerically challenging: the solutions tended to become linearly dependent, so that the computation of the superposition coefficients was dominated by numerical noise. Instead, we started the integration from the stellar surface (with the mass M and radius R previously determined by numerically solving the TOV equations, as discussed in Section 3) up to the crust–core interface. Since we had only two boundary

conditions at the surface (vanishing of the radial and tangential tractions, see [38] for more details), four linearly-independent solutions were generated. At the interface between the hadronic regions with different elements, we applied suitable boundary conditions to deal with the discontinuous change of the shear modulus and of the energy density [38], and pursued the integration up to the crust–core interface. This "inward" solution was matched to the "outward" solution obtained by integrating the equations from the stellar center up to the quark core surface imposing the same boundary conditions.

4.2. Global Structure

We have computed the mass–radius relations of SDs for the different quark-matter EoSs described in Section 2.2. For each EoS, we have considered the two limiting configurations with the crust–core transition pressure $P_{cc} = P_\beta$ and $P_{cc} = P_{drip}$. Note that the latter value might not be strictly reachable [13].

The mass–radius for $P_{cc} = P_{drip}$ and $P_{cc} = P_\beta$ are plotted in Figures 1 and 2, respectively. Comparing SD1 and SD2, we see that the radius increases with $\mathcal{B}$ and a_2 for a given mass. The smallest (largest) radii were obtained for parametrization SQM2 (SS2). For a $0.6M_\odot$ SD, the maximum relative change in R (between the least and the most compact configurations) amounts to 5.9% for $P_{cc} = P_{drip}$, and only 2.1% for $P_{cc} = P_\beta$. In both cases, the central energy density increases by about a factor of 4.3, whereas the radius and the mass of the core each decreases by about 52%. The mass and radius of the core of SDs thus obey similar approximate scaling properties, as originally discussed for bare SSs (see, e.g., Section 8.13 in [34]).

Despite the uncertainties in the quark-matter EoS resulting in large variations in the mass and radius of the quark core, the global structure of SDs remains fairly well-determined. In all cases, SDs are more compact than WDs, although the differences are less pronounced for lower P_{cc} values.

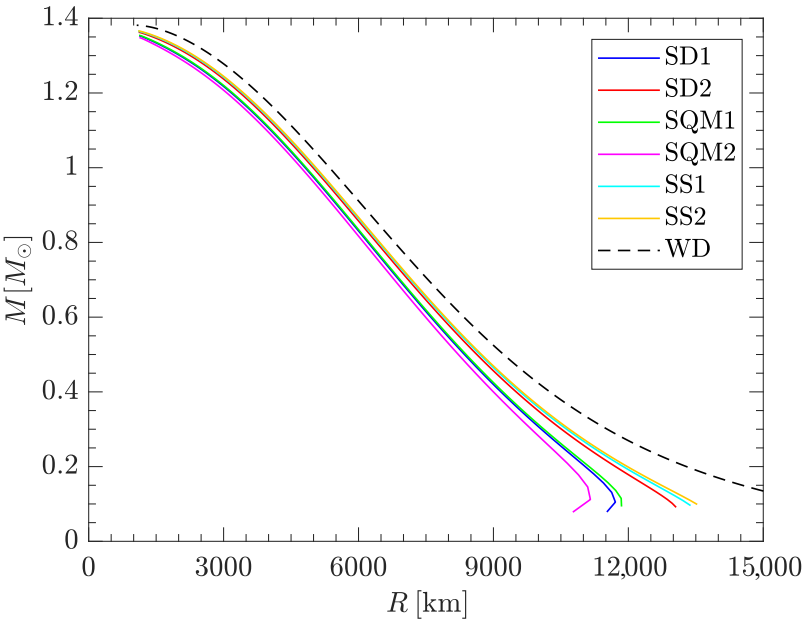

Figure 1. Mass–radius relations for oxygen SDs with $P_{cc} = P_{drip}$. Different EoSs of quark matter are considered: SD1, SD2, SQM1, SQM2, SS1 and SS2 (solid lines). The results are compared with those for oxygen WDs (dashed line).

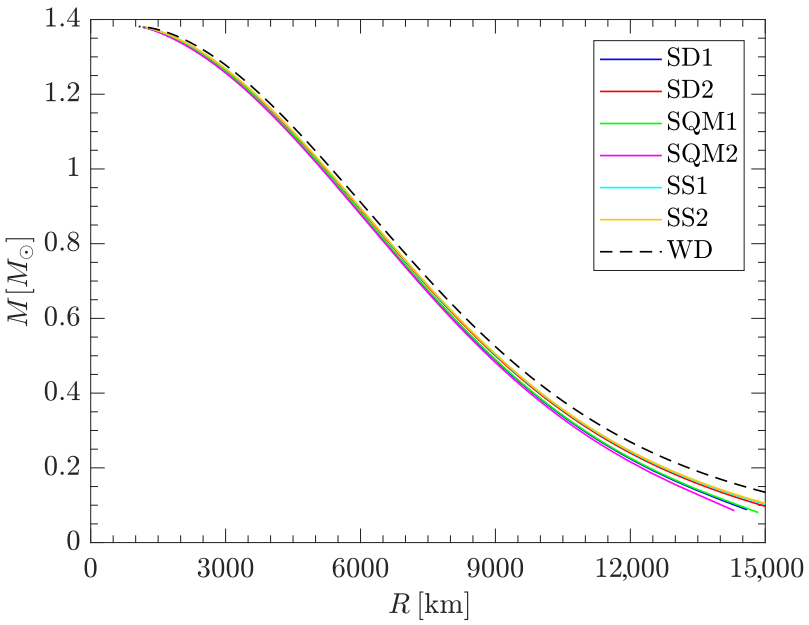

Figure 2. Same as Figure 1 for $P_{\rm cc} = P_\beta$.

4.3. Tidal Deformability

4.3.1. Love Number

We have computed the second gravitoelectric Love number k_2 for the different quark-matter EoSs, taking into account the elasticity of the hadronic envelope and of the core. As shown in [38], the effect of elasticity is to reduce k_2. The largest reduction is, therefore, expected for the largest pairing gap Δ. In Figures 3 and 4, we present k_2 for SDs as a function of their mass with the crust–core transition pressure set to $P_{\rm cc} = P_{\rm drip}$ and $P_{\rm cc} = P_\beta$, respectively. Results for entirely crystallized WDs are also shown for comparison. We see that the variations in k_2 with the EoS are qualitatively similar to those for the radius. For each given EoS, the changes in k_2 due to the variations in Δ in the range 5–25 MeV are contained within the thickness of the corresponding curve. The maximum relative changes in k_2 between the most extreme configurations of a $0.6M_\odot$ SD are about 12% for $P_{cc} = P_{\rm drip}$ and 4.5% for $P_{\rm cc} = P_\beta$, respectively.

For all the SD models considered, k_2 remains smaller than that for WDs.

4.3.2. Screening Effect

Although the crystalline color-superconducting core is extremely dense and rigid, it represents $\sim$0.2% of the stellar radius at most. The screening effects [25,26] induced by the surrounding hadronic envelope are therefore expected to be quite strong. To more precisely assess the importance of these effects, we have calculated the tidal deformability of SDs having the most rigid possible crystalline color-superconducting quark core by setting $\Delta = 25$ MeV, and we have compared the results to those obtained for SDs having a fluid quark core. In both cases, the hadronic envelope is fully crystallized (as considered in [18]). We have found that the cancellation is almost perfect: for SD masses between $0.1M_\odot$ and the maximum mass, k_2 remains unchanged within the precision of our code (up to the ninth digit). The effect of the elasticity of the core can therefore be safely ignored.

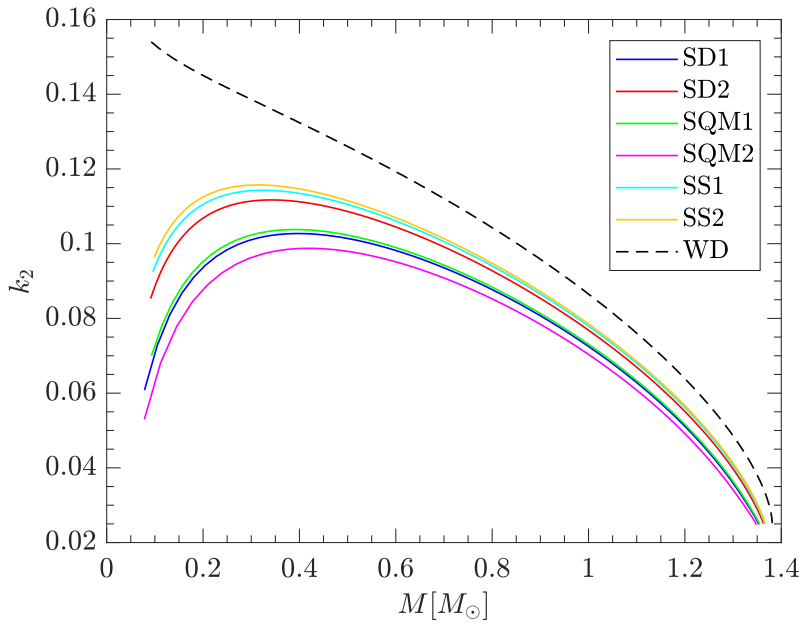

Figure 3. Tidal Love number k_2 of oxygen SDs as a function of the mass M for $P_{cc} = P_{drip}$. Different EoSs of quark matter are considered: SD1, SD2, SQM1, SQM2, SS1 and SS2 (solid lines). Results obtained for a solid or a fluid core are indistinguishable and are compared with those for oxygen WDs (dashed line).

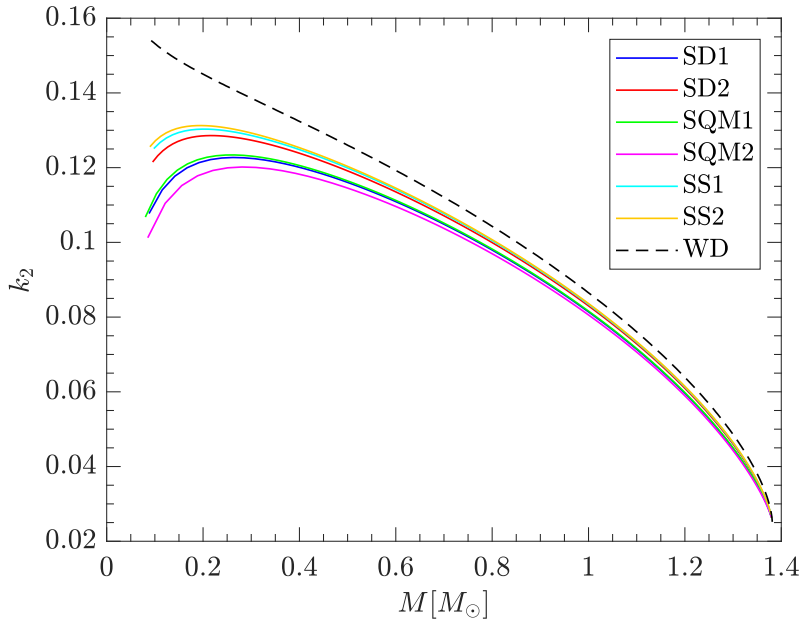

Figure 4. Same as Figure 3 for $P_{cc} = P_\beta$.

4.3.3. Observable Tidal Deformability Parameter

The actual quantity that will be accessible through GW observations is the tidal deformability parameter

$$\Lambda_2 = \frac{2}{3} k_2 \left(\frac{c^2 R}{GM} \right)^5 . \tag{12}$$

The results are plotted in Figures 5 and 6 for $P_{cc} = P_{drip}$ and $P_{cc} = P_\beta$, respectively. Since both R and k_2 are smaller for SDs than for WDs, the reduction in Λ_2 is even larger. The relative reduction in Λ_2 for an entirely elastic $0.6 M_\odot$ SD compared with the corresponding

entirely elastic WD lies between 13% for the SS2 EoS with $P_{cc} = P_\beta$ and 54% for the SQM2 EoS with $P_{cc} = P_{drip}$.

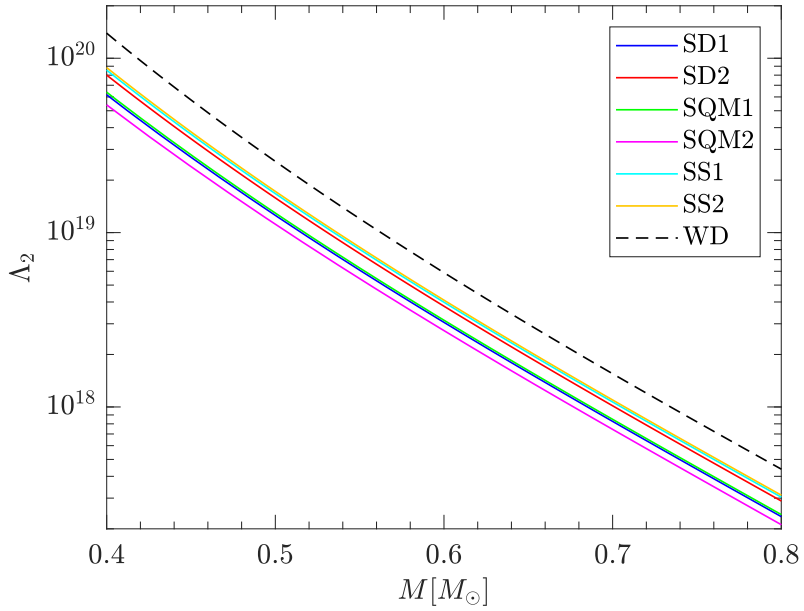

Figure 5. Observable tidal parameter Λ_2 of oxygen SDs as a function of the mass M for $P_{cc} = P_{drip}$. Different EoSs of quark matter are considered: SD1, SD2, SQM1, SQM2, SS1 and SS2 (solid lines). Results obtained for a solid or a fluid core are indistinguishable and are compared with those for oxygen WDs (dashed line).

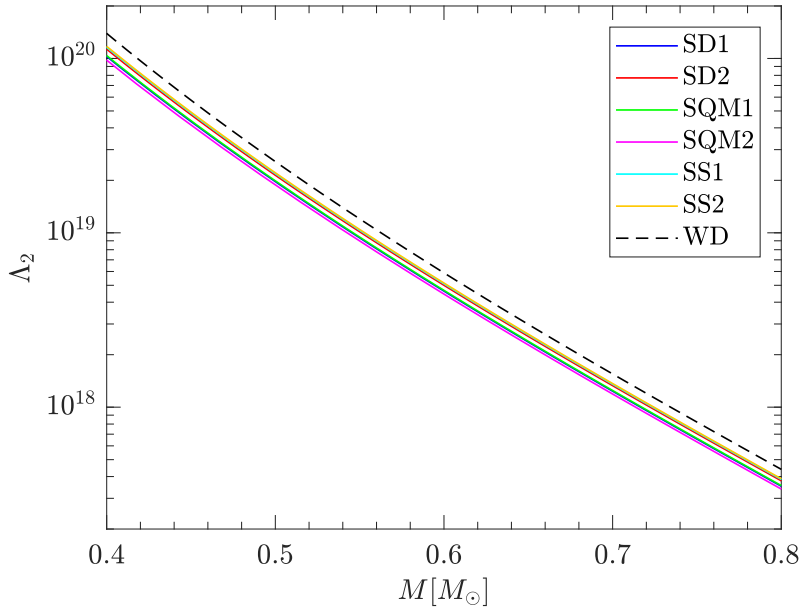

Figure 6. Same as Figure 5 for $P_{cc} = P_\beta$.

5. Conclusions

In this paper, we have pursued our study of SDs [18] by investigating the impact of the quark-matter EoS and crystalline color superconductivity on the structure and tidal deformability of cold-crystallized SDs. For this purpose, we have solved Einstein's equations taking into account the elasticity of both the quark core and the surrounding hadronic envelope using different models of quark matter. We have performed calculations for the whole family of SDs, varying the crust–core transition pressure P_{cc} from the threshold

pressure P_β for the onset of electron captures to the neutron-drip pressure $P_{\rm drip}$. We have focused on oxygen SDs since the role of the hadronic envelope was already studied in our previous work [18].

First, we have found that the uncertainties in the quark-matter EoS only moderately affect the global structure of SDs. Independently of the adopted model for describing the quark core, SDs are more compact than their WD relatives, even when the crust–core transition pressure is set to the lowest possible value P_β. The presence of a quark core in SDs leads to a systematic reduction in the second gravitoelectric Love number k_2 compared with WDs. Although the shear modulus of the crystalline color-superconducting core is two to three orders of magnitude higher than that of the hadronic envelope, its impact on the observable tidal deformability parameter Λ_2 of SDs turns out to be totally negligible: the quark core is almost perfectly screened by the hadronic envelope. Treating the core as a fluid is therefore an excellent approximation—whether the core is actually in a crystalline color-superconducting phase or not.

Despite the uncertainties in the quark-matter EoS, we have found that the observable tidal deformability parameter of SDs can be more than 10% smaller than that of the corresponding WDs, even for the least favorable case $P_{\rm cc} = P_\beta$. Such a deviation is larger than the expected precision of future measurements by the space-based GW detector LISA (see the discussion in [38]). If they exist, SDs potentially hidden among WD binaries could therefore be potentially unmasked through GW observations. On the other hand, measuring Λ_2 alone will not provide any information on whether the core is in a crystalline color-superconducting phase or not.

Author Contributions: Methodology, L.P. and N.C.; software, L.P.; validation, L.P. and N.C.; writing—original draft preparation, L.P. and N.C.; writing—review and editing, L.P. and N.C.; supervision, N.C. All authors have read and agreed to the published version of the manuscript.

Funding: This research was funded by the Fonds de la Recherche Scientifique (Belgium). L.P. is an FRIA grantee of the Fonds de la Recherche Scientifique (Belgium).

Institutional Review Board Statement: Not applicable.

Informed Consent Statement: Not applicable.

Data Availability Statement: Not applicable.

Acknowledgments: The authors thank J.P. Pereira and A. Schmitt for valuable discussions.

Conflicts of Interest: The authors declare no conflict of interest.

Abbreviations

The following abbreviations are used in this manuscript:

NS	Neutron star
SS	Strange star
WD	White dwarf
SD	Strange dwarf
GW	Gravitational wave
LISA	Laser Interferometer Space Antenna
EoS	Equation of state
QCD	Quantum chromodynamics
TOV	Tolman–Oppenheimer–Volkoff

Note

[1] https://physics.nist.gov/cuu/Constants/ (accessed on 14 July 2023).

References

1. Itoh, N. Hydrostatic Equilibrium of Hypothetical Quark Stars. *Prog. Theor. Phys.* **1970**, *44*, 291–292. [CrossRef]
2. Brecher, K.; Caporaso, G. Obese 'neutron' stars. *Nature* **1976**, *259*, 377–378. [CrossRef]
3. Chodos, A.; Jaffe, R.L.; Johnson, K.; Thorn, C.B.; Weisskopf, V.F. New extended model of hadrons. *Phys. Rev. D* **1974**, *9*, 3471–3495. [CrossRef]
4. Witten, E. Cosmic separation of phases. *Phys. Rev. D* **1984**, *30*, 272–285. [CrossRef]
5. Bodmer, A.R. Collapsed Nuclei. *Phys. Rev. D* **1971**, *4*, 1601–1606. [CrossRef]
6. Chin, S.A.; Kerman, A.K. Possible long-lived hyperstrange multiquark droplets. *Phys. Rev. Lett.* **1979**, *43*, 1292–1295. [CrossRef]
7. Terazawa, H. Super-Hypernuclei in the Quark-Shell Model. *J. Phys. Soc. Jpn.* **1989**, *58*, 3555. [CrossRef]
8. Alcock, C.; Farhi, E.; Olinto, A. Strange Stars. *Astrophys. J.* **1986**, *310*, 261. [CrossRef]
9. Alcock, C.; Olinto, A. Exotic Phases of Hadronic Matter and their Astrophysical Application. *Annu. Rev. Nucl. Part. Sci.* **1988**, *38*, 161–184. [CrossRef]
10. Glendenning, N.K.; Kettner, C.; Weber, F. Possible New Class of Dense White Dwarfs. *Phys. Rev. Lett.* **1995**, *74*, 3519–3522. [CrossRef]
11. Glendenning, N.K.; Kettner, C.; Weber, F. From Strange Stars to Strange Dwarfs. *Astrophys. J.* **1995**, *450*, 253. [CrossRef]
12. Alford, M.G.; Harris, S.P.; Sachdeva, P.S. On the Stability of Strange Dwarf Hybrid Stars. *Astrophys. J.* **2017**, *847*, 109. [CrossRef]
13. Clemente, F.D.; Drago, A.; Char, P.; Pagliara, G. Stability and instability of strange dwarfs. *arXiv* **2022**, arXiv:2207.08704.
14. Goncalves, V.P.; Jimenez, J.C.; Lazzari, L. Revisiting the stability of strange-dwarf stars and strange planets. *arXiv* **2023**, arXiv:2301.07654.
15. Alcock, C.; Farhi, E. Evaporation of strange matter in the early Universe. *Phys. Rev. D* **1985**, *32*, 1273–1279. [CrossRef] [PubMed]
16. Bucciantini, N.; Drago, A.; Pagliara, G.; Traversi, S.; Bauswein, A. Formation and evaporation of strangelets during the merger of two compact stars. *Phys. Rev. D* **2022**, *106*, 103032. [CrossRef]
17. Kurban, A.; Huang, Y.F.; Geng, J.J.; Zong, H.S. Searching for strange quark matter objects among white dwarfs. *Phys. Lett. B* **2022**, *832*, 137204. [CrossRef]
18. Perot, L.; Chamel, N.; Vallet, P. Unmasking strange dwarfs with gravitational-wave observations. *Phys. Rev. D* **2023**, *107*, 103004. [CrossRef]
19. Baym, G.; Pethick, C.; Sutherland, P. The Ground State of Matter at High Densities: Equation of State and Stellar Models. *Astrophys. J.* **1971**, *170*, 299. [CrossRef]
20. Alford, M.; Rajagopal, K.; Wilczek, F. Color-flavor locking and chiral symmetry breaking in high density QCD. *Nucl. Phys. B* **1999**, *537*, 443–458. [CrossRef]
21. Alford, M.; Bowers, J.A.; Rajagopal, K. Crystalline color superconductivity. *Phys. Rev. D* **2001**, *63*, 074016. [CrossRef]
22. Matsuzaki, M.; Kobayashi, E. Structure of strange dwarfs with colour superconducting core. *J. Phys. G Nucl. Part. Phys.* **2007**, *34*, 1621–1626. [CrossRef]
23. Anglani, R.; Casalbuoni, R.; Ciminale, M.; Ippolito, N.; Gatto, R.; Mannarelli, M.; Ruggieri, M. Crystalline color superconductors. *Rev. Mod. Phys.* **2014**, *86*, 509–561. [CrossRef]
24. Mannarelli, M.; Rajagopal, K.; Sharma, R. Rigidity of crystalline color superconducting quark matter. *Phys. Rev. D* **2007**, *76*, 074026. [CrossRef]
25. Lau, S.Y.; Leung, P.T.; Lin, L.M. Tidal deformations of compact stars with crystalline quark matter. *Phys. Rev. D* **2017**, *95*, 101302. [CrossRef]
26. Lau, S.Y.; Leung, P.T.; Lin, L.M. Two-layer compact stars with crystalline quark matter: Screening effect on the tidal deformability. *Phys. Rev. D* **2019**, *99*, 023018. [CrossRef]
27. Chamel, N.; Fantina, A.F. Electron exchange and polarization effects on electron captures and neutron emissions by nuclei in white dwarfs and neutron stars. *Phys. Rev. D* **2016**, *93*, 063001. [CrossRef]
28. Lunney, D.; Pearson, J.M.; Thibault, C. Recent trends in the determination of nuclear masses. *Rev. Mod. Phys.* **2003**, *75*, 1021–1082. [CrossRef]
29. Baiko, D.A.; Potekhin, A.Y.; Yakovlev, D.G. Thermodynamic functions of harmonic Coulomb crystals. *Phys. Rev. E* **2001**, *64*, 057402. [CrossRef]
30. Chugunov, A.I. Neutron star crust in Voigt approximation II: general formula for electron screening correction for effective shear modulus. *Mon. Not. R. Astron. Soc.* **2022**, *517*, 4607–4611. [CrossRef]
31. Alford, M.; Braby, M.; Paris, M.; Reddy, S. Hybrid Stars that Masquerade as Neutron Stars. *Astrophys. J.* **2005**, *629*, 969. [CrossRef]
32. Schmitt, A. *Dense Matter in Compact Stars*; Springer: Berlin/ Heidelberg, Germany, 2010; Volume 811. [CrossRef]
33. Mannarelli, M.; Pagliaroli, G.; Parisi, A.; Pilo, L. Electromagnetic signals from bare strange stars. *Phys. Rev. D* **2014**, *89*, 103014. [CrossRef]
34. Haensel, P.; Potekhin, A.Y.; Yakovlev, D.G. *Neutron Stars. 1. Equation of State and Structure*; Springer: New York, NY, USA, 2007.
35. Zdunik, J.L. Strange stars—Linear approximation of the EOS and maximum QPO frequency. *Astron. Astrophys.* **2000**, *359*, 311–315.
36. Dey, M.; Bombaci, I.; Dey, J.; Ray, S.; Samanta, B. Strange stars with realistic quark vector interaction and phenomenological density-dependent scalar potential. *Phys. Lett. B* **1998**, *438*, 123–128. [CrossRef]

37. Hinderer, T. Tidal Love Numbers of Neutron Stars. *Astrophys. J.* **2008**, *677*, 1216–1220. [CrossRef]
38. Perot, L.; Chamel, N. Tidal deformability of crystallized white dwarfs in full general relativity. *Phys. Rev. D* **2022**, *106*, 023012. [CrossRef]